

Novel mutations of the *RS1* gene in a cohort of Chinese families with X-linked retinoschisis

Jieqiong Chen, Ke Xu, Xiaohui Zhang, Zhe Pan, Bing Dong, Yang Li

(The first two authors contributed equally to this work.)

Beijing Institute of Ophthalmology, Beijing Tongren Eye Center, Beijing Tongren Hospital, Capital Medical University, Beijing Ophthalmology & Visual Sciences Key Lab. Beijing, China

Purpose: X-linked retinoschisis is a retinal dystrophy caused by mutations in the *RS1* gene in Xp22.1. These mutations lead to schisis (splitting) of the neural retina and subsequent reduction in visual acuity in affected men (OMIM # 312700). The aim of this study was to identify the *RS1* gene mutations in a cohort of Chinese patients with X-linked retinoschisis, and to describe the associated phenotypes.

Methods: Patients and unaffected individuals from 16 unrelated families underwent detailed ophthalmic examinations. After informed consent was obtained, genomic DNA was extracted from the venous blood of all participants. All exons including the exon-intron boundaries of the *RS1* gene, were amplified by PCR and the products were analyzed by direct sequencing. Long-range PCR followed by DNA sequencing was used to define the breakpoints of the large deletion.

Results: Sixteen male individuals from 16 families were diagnosed with retinoschisis by clinical examination. The median age at review was 13.2 years (range: 5–34 years); the median best-corrected visual acuity upon review was 0.26 (range 0.02–1.0). Foveal schisis was found in 82.8% of the eyes (24/29) while peripheral schisis was present in 27.5% of the eyes (8/29). Sequencing of the *RS1* gene identified 16 mutations, nine of which were novel. The mutations included eight missense mutations, all located in exons 4–6 (50.0%), two nonsense mutations (12.5%), four small deletions or insertions (25.0%), one splice site mutation (6.25%), and one large genomic deletion that included exon1 (6.25%).

Conclusions: The mutations found in our study broaden the spectrum of *RS1* mutations. The identification of the specific mutation in each pedigree will allow future determination of female carrier status for genetic counseling purposes.

X-linked retinoschisis (XLRS) is one common cause of juvenile macular degeneration in males, with a worldwide prevalence ranging from 1:5,000 to 1:25,000 [1]. The predominant clinical features include early onset visual loss, as well as bilateral foveal schisis, which is characterized by radiating cystic-like changes within the inner retinal layers of the macular region. Peripheral schisis, usually located in the inferotemporal retina, occurs in less than 50% of affected individuals [2,3]. The most common sight-threatening complications of XLRS include vitreous hemorrhage in 4–20% of affected individuals and retinal detachment in 5–22% of cases [3]. Typical electroretinograms (ERGs) of XLRS-affected individuals reveal reduced b-wave amplitude with relative preservation of the a-wave amplitude; however, the ERG response is more variable than previously expected [4].

Optic coherence tomography (OCT) is a relatively new and effective method for obtaining high-resolution cross-sectional images of the neurosensory retina. OCT of XLRS

patients indicates that foveomacular schisis occurs predominantly at the inner nuclear layer, occasionally at the outer nuclear layer/outer plexiform layer, and only rarely at the nerve fiber layer [5].

XLRS is an X-linked recessive disease, with almost full penetrance, but it exhibits a high degree of intra- and inter-familial variability [1–3]. The only disease causative gene of XLRS is the *XLRS1* (or *RS1*) gene located on chromosome Xp22.2 [6]. This gene contains six exons and encodes a 224 amino acid protein known as retinoschisin. The 24 kDa protein consists of a 23 amino acid N-terminal leader sequence, a 39 amino acid RS1 domain, a 157 amino acid discoidin domain, and a five amino acid C-terminal segment. The discoidin domain, encoded by exons 4–6, is the main structural feature of retinoschisin and is highly conserved across species [6,7]. Retinoschisin is a cell adhesion protein that plays a crucial role in maintaining the structural integrity of the retina [7].

To date, more than 200 mutations have been identified in the *RS1* gene and more than half of these are missense mutations. The other disease-causing mutations include nonsense mutations, splicing site defects, deletions, and insertions [6–19]. No significant correlations have been found between

Correspondence to: Yang Li, Beijing institute of Ophthalmology, Beijing Tongren Hospital, Hougou Lane 17, Chong Nei Street, Beijing, 100730, China; Phone: 8610-58265915; FAX: 8610-65288561 or 65130796; email: yilibio@163.com

TABLE 1. PRIMERS USED IN SEQUENCING OF THE RSI GENE AND ALLELE-SPECIFIC PCR ANALYSIS.

| Exon/mutation site | Primer sequence (5'-3') | Size (bp) | TM (°C) |
|--------------------|---|-----------|---------|
| 1 | F:TCTTCCATGAGACTTCCTTGTTGA R:AGATTTCGAGACCCATCCTGTT | 485 | 60 |
| 2 | F:TCTTCCATGAGACTTCCTTGTTGA R:TACATTAAAAACAAAGTGATAGTCCTC | 249 | 58 |
| 3 | F:CCAGGGTGGCAGACATTTT R:GGTAGCGTTCAGGGGGTT | 406 | 60 |
| 4 | F:TTCTTTTACTTCATCCTTCATTCC R:CTCACTGTAACCTCCGCTTCC | 550 | 60 |
| 5 | F:GCAGGGAGAGGGAGAATGAGA R:CCAAAGCAAGCCCAGGAA | 570 | 60 |
| 6 | F:CAGTTCCAGATGTCCCAAGCA R:TGTCCATCTCGGTGGTGTGTG | 432 | 62 |
| 5/p.Y151H | R: TCCTGTACTGCACGCTGa G | 347 | 60 |
| 5/p.Y166H | R:TTCCAGTCTGGTCCTTGa G | 392 | 60 |
| 5/p.K167E | R:GTTGTTTCCAGTCTGGTCCa C | 397 | 60 |
| 6/p.I194N | R:CGGATGAAGCGGGAGATGT | 271 | 62 |

Abbreviations: F: forward; R: reverse; primer sequences with lower case indicate modified nucleotides to specifically amplify the mutant sequence; red, mutation-specific nucleotide.

genotype and phenotype in previous studies, except for one recent study by Vincent et al., where mild ERG abnormalities were reported to be more commonly associated with missense changes [19].

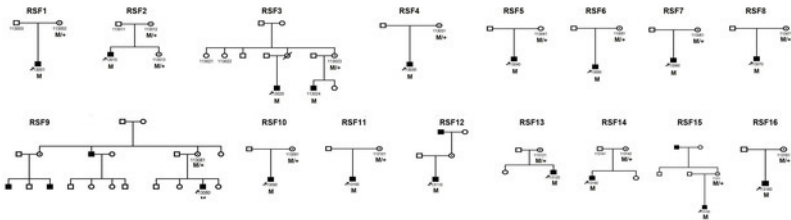
In the present study, we performed mutation screening of the *RS1* gene in a cohort of affected individuals with XLRS. Fifteen intragenic mutations and a large deletion were identified in this cohort of patients. Nine of these mutations are novel. No correlation between genotype and phenotype was revealed in this study.

METHODS

Clinical studies: This study was approved by the Beijing Tongren Hospital Joint Committee on Clinical Investigation and was performed in accordance with the tenets of the

Declaration of Helsinki. Sixteen families with XLRS were recruited for this study. After informed consent was obtained, each proband underwent clinical examinations, including best-corrected visual acuity (BCVA) using E decimal charts, slit-lamp biomicroscopy, fundus examination and photography, single-flash ERG, and OCT. The diagnostic criteria in XLRS individuals included a history of bilateral visual impairment at or before school age, radiating cystic-like changes in the macular region, blunted foveal reflex with or without peripheral lesions, and a decreased ERG b-wave.

Detection of mutations in the RSI gene: Peripheral blood samples were collected from all the participants by venipuncture in heparinized collecting tubes and stored at 4 °C for less than 1 week. Genomic DNA was extracted from peripheral blood leukocytes using a genomic DNA extraction



solid symbols indicate affected; open symbols indicate unaffected; open symbols with a spot indicate carrier; arrows below symbols indicate proband; M indicates mutant; + indicates wild-type.

Figure 1. Pedigrees of the families with retinoschisis showed some families with an X-linked recessive pattern. Pedigrees of the families with retinoschisis. Squares indicate males; circles indicate females; slashed symbols indicate deceased;

TABLE 2. CLINICAL FEATURES AND RESULTS OF THE RSI GENE MUTATIONS SCREENING IN THE STUDY.

| Patient ID | Gender | Age(year) | | BCVA | | Macular retinoschisis | | Peripheral retinoschisis | | Other complication | ERG | Identified mutations | Exon | Source |
|------------|--------|-----------|-------|------|------|-----------------------|------|--------------------------|-----|-------------------------------------|-------------------------------------|-----------------------------|------|--------|
| | | exam | onset | OD | OS | OD | OS | OD | OS | | | | | |
| 113001 | M | 15 | EC | 0.1 | 0.1 | YES | YES | YES | YES | NO | NA | c.370C>T p.Q124X | 5 | Novel |
| 113010 | M | 6 | 4 | 0.4 | 0.5 | YES | YES | NO | NO | NO | NA | c.330delT.p.C110fs+15X | 5 | Novel |
| 113020 | M | 24 | 8 | 0.1 | 0.05 | YES | NA | YES | NA | cataract (OU), exotropia and RD(OS) | NA | c.581T>A p.I194N | 6 | Novel |
| 113030 | M | 8 | 8 | 0.25 | 0.3 | YES | YES | NO | NO | NO | NA | c.98G>A p.W33X | 3 | Novel |
| 113040 | M | 8 | 6 | 0.4 | 0.4 | YES | YES | NO | NO | NO | reduced photopic and 30Hz responses | del exon 1 | 1 | [8] |
| 113050 | M | 6 | EC | 0.5 | 0.02 | NO | NO | YES | YES | NO | NA | c.78+5G>T | 2 | Novel |
| 113060 | M | 5 | 5 | 0.2 | 0.1 | YES | YES | YES | YES | NO | NA | c.638G>A p.R213Q | 6 | [9] |
| 113070 | M | 5 | 3 | 0.2 | 0.1 | YES | YES | NO | NO | NO | NA | c.578C>T p.P193L | 6 | [8] |
| 113080 | M | 34 | EC | 0.2 | 0.2 | YES | YES | NO | NO | NO | NA | c.599G>A p.R200H | 6 | [8] |
| 113090 | M | 5 | 5 | 0.4 | HM | YES | NA | NO | NA | RD (OS) | NA | c.52+2_3 ins tgaaggt | 1 | Novel |
| 113100 | M | 6 | 6 | 0.05 | 1.0 | NA | NO | NA | YES | exotropia and VH(OD) | b-wave reduced | c.496T>C p.Y166H | 5 | Novel |
| 113110 | M | 41 | EC | 0.3 | 0.15 | MA | MA | NO | NO | NO | NA | c.451T>C p.Y151H | 5 | Novel |
| 113120 | M | 9 | 8 | 0.1 | 0.2 | YES | YES | NO | NO | NO | NA | c.499A>G p.K167E | 5 | Novel |
| 113140 | M | 7 | EC | 0.3 | 0.2 | YES | YES | NO | NO | NO | NA | c.208G>A p.G70S | 4 | [8] |
| 113150 | M | 4 | 4 | 0.02 | 0.4 | YES | YES | NO | NO | NO | NA | c.375_378delAGATp.I125fs+1X | 5 | [8] |
| 113160 | M | 27 | EC | 0.06 | 0.06 | YES* | YES* | NO | NO | nystagmus (OU) | b-wave reduced | c.489del G p.W163fsX | 5 | [13] |

Abbreviations: M, male; OD, right eye; OS, left eye; EC, early childhood; OU, both eyes; RD, retinal detachment; VH, vitreous hemorrhage; NA, data not available; MA, macular atrophy; *, large retinoschisis cavity.

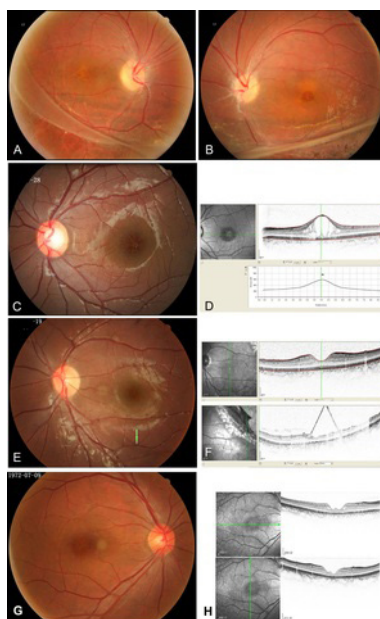


Figure 2. Fundus photography and optical coherence tomography images of patients. **A** and **B**: Fundus appearance of patient 113001 shows foveal and peripheral retinal schisis in both eyes. **C**: Fundus photograph of the left eye of patient 113010 shows a typical cystic-like foveal schisis. **D**: His optical coherence tomography (OCT) images show foveomacular schisis within the inner nuclear layer of the retina. **E**: Fundus photograph of the left eye of patient 113100 shows normal foveal reflexes and a peripheral schisis cavity (arrow). **F**: OCT images of patient 113100 show normal macular structure (top) and peripheral retinal schisis of the

inner retina (bottom). **G**: Fundus photography of the right eye of patient 110110 shows absent foveal reflexes. **H**: His OCT images present macular atrophy.

and purification kit (Vigorous Whole Blood Genomic DNA Extraction Kit, Vigorous Beijing, China), according to the manufacturer's protocol. In briefly, whole erythrocytes were lysed with the lysis buffer and white cells pellets were extracted, then DNA was extracted from the pellets using lysis buffer, washing buffer, and solving buffer. The coding regions and the exon-intron boundaries of the *RS1* gene were amplified by PCR in the patients from the 16 families using the primers described in Table 1. PCR assays were performed using standard reaction mixtures and purified PCR products were directly sequenced on an ABI Prism 373A DNA sequencer (Applied Biosystems, Foster City, CA). Nucleotide sequences were compared with the published cDNA sequence of *RS1* (GenBank [NM_000330.3](#)). For the *RS1* gene, cDNA numbering +1 corresponds to A in the ATG translation initiation codon in *RS1*.

Allele-specific polymerase chain reaction analysis: Allele-specific PCR analysis was performed in the available family members and in 100 normal controls to confirm the variations found in the sequencing. Allele-specific reverse primers in exon5 and exon6 of the *RS1* gene are described in Table 1. The PolyPhen (Polymorphism Phenotyping) program was used to predict the potential functional impact of an amino acid change [20].

RESULTS

Clinical findings: Twenty-two male individuals from the 16 families were diagnosed with retinoschisis by clinical examination and family history review (Figure 1). Of the 22 affected individuals, 16 probands were evaluated; their clinical features are summarized in Table 2. Eleven of the 16 (11/16) probands had been diagnosed in their first decade and the median age at diagnosis was 13.1 years (range 4–41 years). The BCVA at the time of diagnosis ranged from 1.0 to hand movement. Retinal findings varied considerably. Twelve patients (22 eyes) presented a typical cystic-like foveal schisis, while three patients (5 eyes) also had peripheral retinal schisis (Figure 2A-D). Patients 113050 and 113100 had only peripheral retinal schisis (Figure 2E). Patient 113100 had 1.0 visual acuity and his OCT images revealed peripheral schisis cavities but failed to show any evidence of foveal cystic changes (Figure 2F). His left eye had visual acuity only for hand movement due to a recent spontaneous vitreous hemorrhage. Foveal atrophy was revealed in one elder proband (>40 year old) through his fundus photography and OCT findings (Figure 2 G,H). In addition to the typical clinical features of XLRS, this cohort of patients also exhibited retinal detachment, vitreous hemorrhage, strabismus, and cataract.

The clinical features of patient 113160 are worthy of further description. The 27-year-old man had bilateral poor vision and nystagmus in his early childhood. Because of his local clinic's constraints, he was initially diagnosed with optic

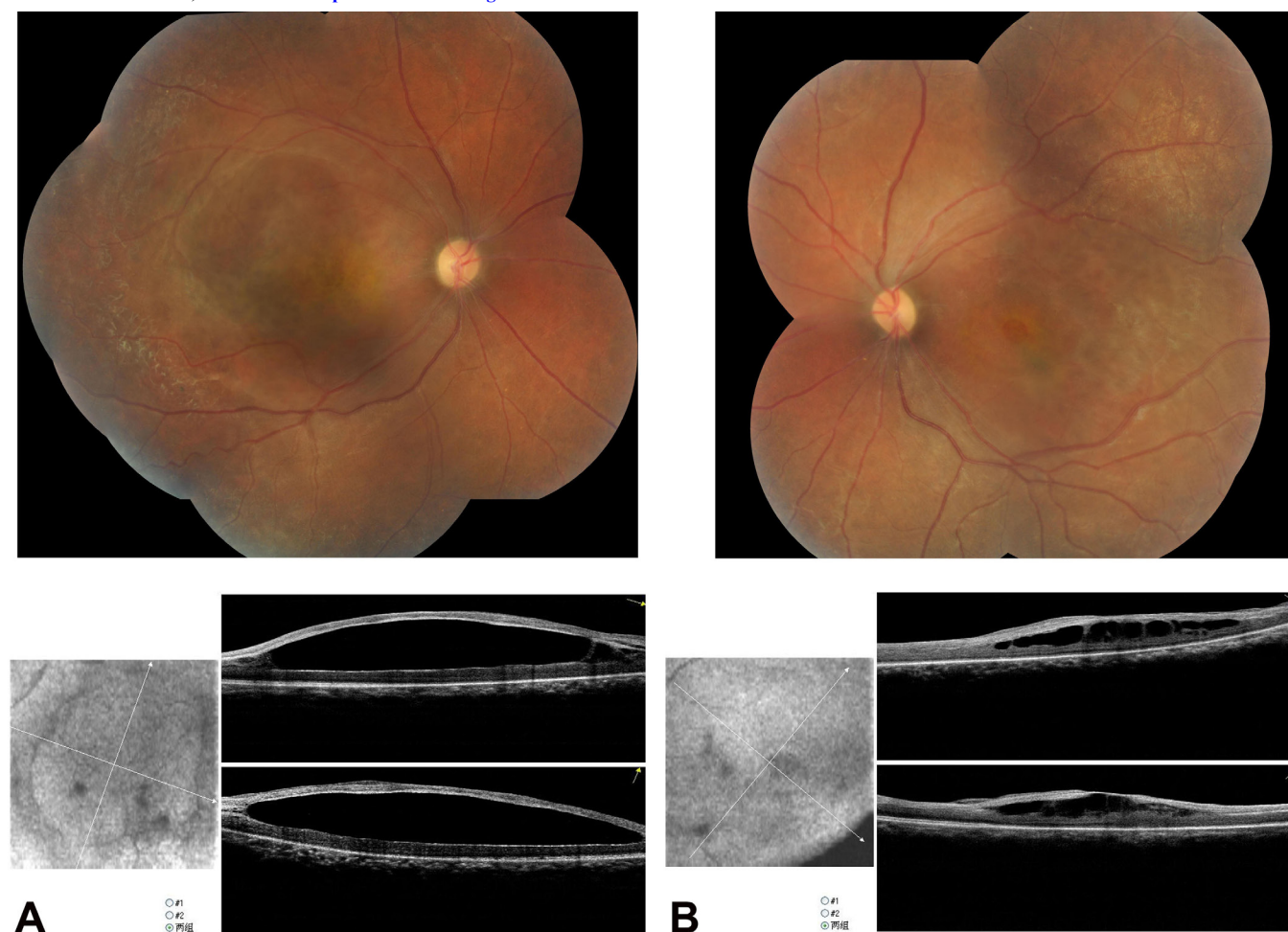


Figure 3. Fundus photography and optical coherence tomography images of patient 113160. **A:** Fundus photography (top) and optical coherence tomography (OCT) image (bottom) of the right eye of patient 113160 shows an unusually large retinoschisis cavity. **B:** His fundus photography (top) and OCT image (bottom) of the left eye.

atrophy and sent to our laboratory for the related molecular analysis. His fundus examination showed temporal pallor of the optic discs, a large elevated mound in the posterior pole with a size of over 5 disk diameters, and pigmentary changes in the peripheral retina (Figure 3). His OCT scanning revealed two unusually large retinoschisis cavities in both eyes, which corresponded to the large elevated area observed in his fundus (Figure 3). His ERG testing showed a “negative” ERG response with the b-wave amplitude severely decreased and the a-wave mildly decreased.

Mutation analysis: Sequencing the *RS1* gene identified 16 mutations in this cohort of Chinese families with XLRS. Each mutation was found only once and nine were detected for the first time in this study (Table 2). All patients carried hemizygous mutations, while their mothers harbored the heterozygous mutations (Figure 1). The mutations included eight missense mutations: c.451T>C (p.Y151H), c.496T>C(p.

Y166H), c.578C>T(p.P193L), c.581T>A(p.I194N), c.599G>A(p.R200H), c.638G>A(p.R213Q), and c.499A>G (p.K167E) c.208G>A(p.G70S; Figure 4A); two nonsense mutations: c.98G>A(p.W33X), c.370C>T(p.Q124X); one splicing defect: c.78 +5G>T; one small insertion: c.52+2–3 ins tgaaggt; three deletion-reduced frameshifts: c.330delT (p.C110fs+15X), c. 375_378del AGAT (p.Ile125fs+1X), and c.489del G (p. W163fsX); and one large deletion that included the entire exon 1. Allele-specific PCR analyses showed that the novel mutations cosegregated with the phenotype in the cohort patients, and none of the mutations were detected in 100 normal controls. The PolyPhen program analysis predicted that four of the novel missense mutations (p.Y151H, p.Y166H, p.K167E, and p.I194N) were probably damaging. The large genomic deletion was detected by the failure of amplification of exon 1 for proband 113040. This deletion is at least 9,174 bp (from 955 bp upstream of the exon1 splice

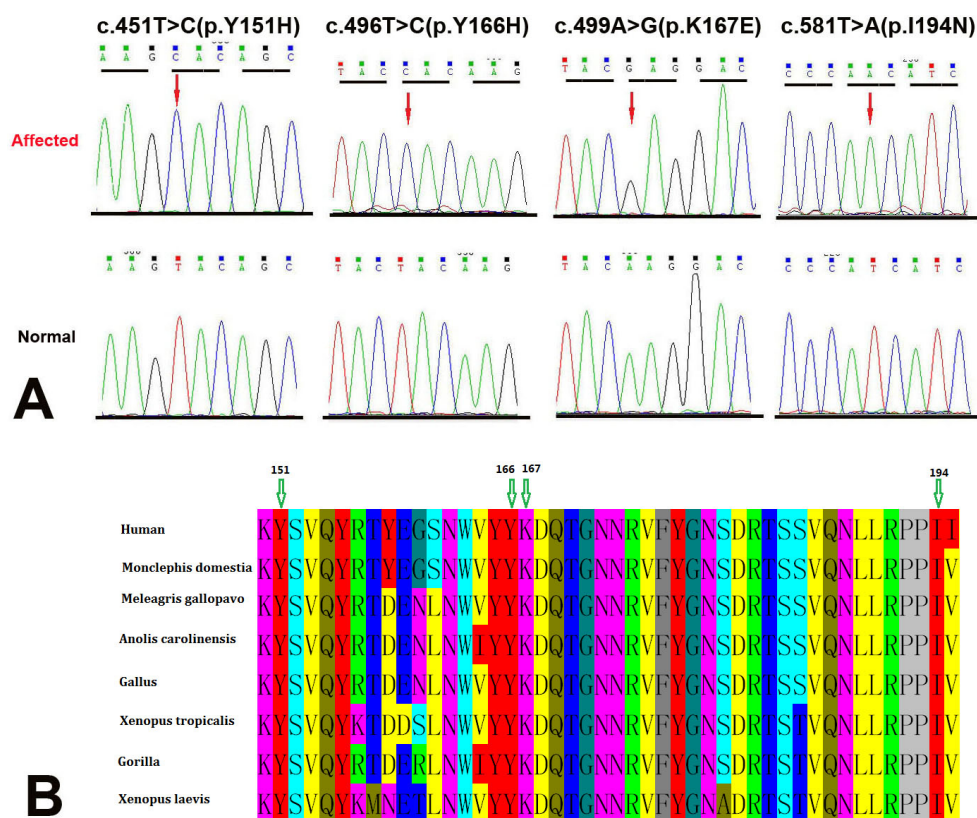


Figure 4. DNA sequence chromatograms and sequence alignment of portion of the discoidin domain spanning the novel missense mutations with other species. **A:** The DNA sequence chromatograms (sense strand) shows four novel missense mutations: c.451T>C (p.Y151H), c.496T>C (p.Y166H), c.499A>G (p.K167E), and c.581T>A (p.I194N) (top) and the corresponding wild-type sequences (bottom). **B:** Multiple species sequence alignment of the portion of the discoidin domain that spans the four novel missense mutations showed the mutations site (arrow) are highly conserved.

acceptance site to 8,132 bp downstream of the exon splice donor site); however, we were unable to perform an exact size estimation or breakpoint characterization of the large deletion due to the inability to amplify across this region in both the patient and the healthy individuals.

DISCUSSION

In this study, we screened *RS1* mutations from 16 patients belonging to 16 Chinese families and evaluated the genotype and phenotype correlation between these patients. Sixteen different mutations were identified, nine of which have not been previously reported. No obvious genotype-phenotype association was observed in this small cohort of Chinese patients.

The majority of the *RS1* mutations detected in this study were missense mutations (8/16), although nonsense mutations (2/16), a splicing site mutation (1/16), small insertion or deletion (4/16), and a large deletion (1/16) were all detected. In agreement with previously published XLRs studies, the mutations found in this study were not distributed randomly over the gene. Eight missense mutations were located in exons 4–6; these encode the discoidin domain, which extends from residue 63 to residue 219. The remaining seven mutations,

which resulted in premature translation termination, were scattered in exon 5, etc which encode the leader sequence (residues 1–23) and the RS1 domain (residues 24–62). Only one mutation was identified in exon4 in this study (exon4: 6.3%; exon5: 43.8%; exon6: 25.0%), in contrast to the data from the Retinoschisis Database ([[dmd](#)]; exon 4: 42.7%; exon 5: 16.3%; exon 6: 26.9). This may reflect the relatively small number of patients in our study.

The four novel missense mutations were all located in the discoidin domain and residues (Y151, Y166, K167, and I194), which are highly conserved among different species (Figure 4B). These novel mutations may result in protein misfolding and intracellular retention by the endoplasmic reticulum (ER) quality control system. One large genomic deletion around exon1 was detected in family RSF5. This deletion is more than 9,174 bp and should include the promoter region of the *RS1* gene; therefore, the deletion may lead to a nonfunctioning null allele or total absence of retinoschisin. At present, about 20 large genomic deletions have been reported and most of these involve exon1 [8,21–24].

The spectrum of *RS1* mutations found in this study is relatively broad, as each patient from the different families carried his own individual mutation. No significant genotype

and phenotype correlation could be observed in this study. The 16 Chinese XLRS families recruited in this study showed considerable heterogeneity in the clinical severity of the disease, with BCVA ranging from hand movement to 1.0 (20/20), and a wide variation was observed between both eyes in each patient. One limitation of this study is that only one patient from each family was clinically evaluated; thus, there is no way to compare the clinical features of patients with the same mutations. Patient 113040 that harbored the exon1 deletion showed a mild clinical phenotype, with a BCVA of 0.4. Fundal examination revealed bilateral spoke-wheel-like retinoschisis involving the maculae. In contrast to this patient, a patient with an exon1 deletion reported by Chan et al. presented clinical features of greater severity, including both foveal and peripheral retinoschisis associated with inferior retinal detachment [22].

In conclusion, we have broadened the mutation spectrum for XLRS by identifying 16 mutations of the *RS1* gene. This type of molecular analysis can provide a molecular diagnosis, especially for atypical cases such as in the very young or elderly XLRS patients. Molecular genetic analysis is very important when it comes to identifying carriers, who usually do not have any symptoms; timely genetic counseling may be helpful in family planning decisions.

ACKNOWLEDGMENTS

We thank the patients and their families for their participation in this study. The study was supported by National Natural Science Foundation of China (No. 81,170,878). The funding organization had no role in the design or conduct of this research.

REFERENCES

- Molday RS, Kellner U, Weber BH. X-linked juvenile retinoschisis: clinical diagnosis, genetic analysis, and molecular mechanisms. *Prog Retin Eye Res* 2012; 31:195-212. [PMID: 22245536].
- Sikkink SK, Biswas S, Parry NRA, Stanga PE, Trump D. X-linked retinoschisis: an update. *J Med Genet* 2007; 44:225-32. [PMID: 17172462].
- Tantri A, Vrabec TR, Cu-Unjieng A, Frost A, Annesley WH, Donoso LA. X-Linked retinoschisis: A clinical and molecular genetic review. *Surv Ophthalmol* 2004; 49:214-30. [PMID: 14998693].
- Renner AB, Kellner U, Fiebig B, Cropp E, Foerster MH, Weber BHF. ERG variability in X-linked congenital retinoschisis patients with mutations in the *RS1* gene and the diagnostic importance of fundus autofluorescence and OCT. *Doc Ophthalmol* 2008; 116:97-109. [PMID: 17987333].
- Yu J, Ni Y, Keane PA, Jiang C, Wang W, Xu G. Foveomacular schisis in Juvenile X-Linked retinoschisis: An optical coherence tomography study. *Am J Ophthalmol* 2010; 149:973-8. [PMID: 20430364].
- Sauer CG, Gehrig A, Warneke-Wittstock R, Marquardt A, Ewing CC, Gibson A, Lorenz B, Jurklies B, Weber BH. Positional cloning of the gene associated with X-linked juvenile retinoschisis. *Nat Genet* 1997; 17:164-70. [PMID: 9326935].
- Molday RS. Focus on molecules: retinoschisin (RS1). *Exp Eye Res* 2007; 84:227-8. [PMID: 16600216].
- The Retinoschisis Consortium. Functional implications of the spectrum of mutations found in 234 cases with X-linked juvenile retinoschisis. The Retinoschisis Consortium. *Hum Mol Genet* 1998; 7:1185-92. [PMID: 9618178].
- Hotta Y, Fujiki K, Hayakawa M, Ohta T, Fujimaki T, Tamaki K, Yokoyama T, Kanai A, Hirakata A, Hida T, Nishina S, Azuma N. Japanese juvenile retinoschisis is caused by mutations of the *XLRS1* gene. *Hum Genet* 1998; 103:142-4. [PMID: 9760195].
- Pimenides D, George ND, Yates JR, Bradshaw K, Roberts SA, Moore AT, Trump D. X-linked retinoschisis: clinical phenotype and *RS1* genotype in 86 UK patients. *J Med Genet* 2005; 42:e35. [PMID: 15937075].
- Hewitt AW, Fitzgerald LM, Scotter LW, Mulhall LE, McKay JD, Mackey DA. Genotypic and phenotypic spectrum of X-linked retinoschisis in Australia. *Clin Experiment Ophthalmol* 2005; 33:233-9. [PMID: 15932525].
- Shukla D, Rajendran A, Gibbs D, Suganthalakshmi B, Zhang K, Sundaresan P. Unusual manifestations of X-Linked retinoschisis: clinical profile and diagnostic evaluation. *Am J Ophthalmol* 2007; 144:419-23. [PMID: 17631851].
- Li X, Ma X, Tao Y. Clinical features of X linked juvenile retinoschisis in Chinese families associated with novel mutations in the *RS1* gene. *Mol Vis* 2007; 13:804-12. [PMID: 17615541].
- Lesch B, Szabo V, Kanya M, Somfai GM, Vamos R, Varsanyi B, Pamer z, Knezy K, Salacz G, Janaky M, Ferencz M, Hargitai J, Papp A, Farkas A. Clinical and genetic findings in Hungarian patients with X-linked juvenile retinoschisis. *Mol Vis* 2008; 14:2321-32. [PMID: 19093009].
- Riveiro-Alvarez R, Trujillo-Tiebas MJ, Gimenez-Pardo A, Garcia-Hoyos M, Lopez-Martinez MA, Aguirre-Lamban J, Garcia-Sandoval B, Vazquez-Fernandez del Pozo S, Cantalapiedra D, Avila-Fernandez A, Baiget M, Ramos C, Ayuso C. Correlation of genetic and clinical findings in Spanish patients with X-linked Juvenile retinoschisis. *Invest Ophthalmol Vis Sci* 2009; 50:4342-50. [PMID: 19324861].
- Kim SY, Ko HS, Yu YS, Hwang JM, Lee JJ, Kim SY, Kim JY, Seong MW, Park KH, Park SS. Molecular genetic characteristics of X-linked retinoschisis in Koreans. *Mol Vis* 2009; 15:833-43. [PMID: 19390641].
- Xu F, Xiang H, Jiang R, Dong F, Sui R. Phenotypic expression of X-linked retinoschisis in Chinese families with mutations

- in the RS1 gene. *Doc Ophthalmol* 2011; 123:21-7. [PMID: 21701876].
18. Yi J, Li S, Jia X, Xiao X, Wang P, Guo X, Zhang Q. Novel RS1 mutations associated with X-linked juvenile retinoschisis. *Int J Mol Med* 2012; 29:644-8. [PMID: 22245991].
19. Vincent A, Robson AG, Neveu MM, Wright GA, Moore AT, Webster AR, Holder GE. A phenotype–genotype correlation study of X–Linked retinoschisis. *Ophthalmology* 2013; 120:1454-1464. [PMID: 23453514].
20. Ramensky V, Bork P, Sunyaev S. Human non-synonymous SNPs: server and survey. *Nucleic Acids Res* 2002; 30:3894-900. [PMID: 12202775].
21. Huopaniemi L, Tynismaa H, Rantala A, Rosenberg T, Alitalo T. Characterization of two unusual RS1 gene deletions segregating in Danish retinoschisis families. *Hum Mutat* 2000; 16:307-14. [PMID: 11013441].
22. Chan WM, Choy KW, Wang J, Lam DSC, Yip WWK, Fu W, Pang CP. Two cases of X-linked juvenile retinoschisis with different optical coherence tomography findings and RS1 mutation. *Clin Experiment Ophthalmol* 2004; 32:429-32. [PMID: 15281981].
23. Yu P, Li J, Li R, Zhang W. Identification of mutation of the X- linked juvenile retinoschisis gene. *Zhonghua Yi Xue Yi Chuan Xue Za Zhi* 2001; 18:88-91. [PMID: 11295123].
24. Gao L, Zhou J, Wang Y, Jiang D, Chen P, Shi X, Tang L, Zhong Y. Identification of mutation of the X-linked juvenile retinoschisis gene. *Chin J Ocul Fundus Dis* 2004; 3:149-51. .

Articles are provided courtesy of Emory University and the Zhongshan Ophthalmic Center, Sun Yat-sen University, P.R. China. The print version of this article was created on 31 January 2014. This reflects all typographical corrections and errata to the article through that date. Details of any changes may be found in the online version of the article.